Pronounced Visibility of Cerebral Venous Vasculature in Small Vessel Disease; A Susceptibility-weighted Imaging Study

Farhang F Jalilian[1,2], David E Crane[1], FuQiang Gao[1], Sandra E Black[1,3], and Bradley J MacIntosh[1,2]

[1]Heart and Stroke Foundation Canadian Partnership for Stroke Recovery, Sunnybrook Research Institute, Toronto, ON, Canada, [2]Medical Biophysics, University of Toronto, Toronto, ON, Canada, [3]Division of Neurology, Faculty of Medicine, University of Toronto, Toronto, ON, Canada

Introduction: Cerebral Small Vessel Disease (SVD) is the most prevalent neurological condition among elderly adults and is associated with an increased risk of stroke and dementia [1]. SVD manifests as regions of white matter hyperintensity (WMH) on fluid attenuated inversion recovery (FLAIR) images. While SVD is thought to be a vascular problem and ischemic in nature, very little is known about the role of venous vasculature in this condition. Some argue that collagen builds up in veins as SVD progresses [2], which could restrict perfusion to upstream white matter tissue. Among venography techniques, susceptibility-weighted magnetic resonance imaging (SWI) has gained popularity over the past decade [3] and may therefore be useful in the context of assessing SVD severity. The ability of SWI to enable visualization of deep medullary venule in the periventricular white matter has received special attention in a number of clinical applications such as multiple sclerosis (MS) and hypoxic-ischemic disorders [4,5]. While quantitative methods using SWI venography have shown a decrease in venous vasculature visibility in MS patients [4], similar investigations of venous vasculature in other disorders are often limited to qualitative approaches. In particular, no SWI study to date has investigated SVD. The aim of the current study is to examine the role that SWI can play in understanding SVD by developing an automated and quantitative procedure that can isolate venous anatomy. We hypothesize that the number of veins detected on SWI, which may reflect widening related to venous wall pathology will correlate positively to periventricular SVD lesion volume.

Materials and Methods: 32 subjects (mean age 70.7±11.3 years) were scanned on a Philips 3.0T Achieva MRI system at the Sunnybrook Research Institute. They had moderate to severe SVD, either as spontaneous WMHs in the elderly or as Cerebral Autosomal-Dominant Arteriopathy with Subcortical Infarcts and Leukoencephalopathy (CADASIL) in middle-aged individuals. T1-weighted, FLAIR and SWI images were obtained for tissue segmentation, WMHs quantification and venous segmentation, respectively. FLAIR images were acquired with TE/TR=125/9000ms, flip angle=90° and voxel dimensions of 1x1.1x3 mm^3. Imaging parameters for SWI were: TE/TR=41/29 ms, flip angle=15° and voxel dimensions of 0.48x0.48x2.8 mm^3. FLAIR images were automatically segmented using the Fuzzy Lesion EXtractor algorithm to delineate the WMH lesions [6]. SWI images were used to segment veins. This procedure was implemented in MATLAB using a 2-D multiscale vessel-enhancement filtering algorithm [7] that enhanced the vessel-like structures. This was followed by a global thresholding to obtain binary images of venous structures in each axial slice of the SWI images. Lastly, T1-weighted images were segmented to obtain white matter (WM), grey matter (GM) and cerebrospinal fluid masks using FMRIB's Automated Segmentation Tool [8]. The WM region of interest (ROI) was subdivided into normal appearing white matter (NAWM) and WMHs. The periventricular WMH lesion volumes were calculated for each individual and normalized to take into account the periventricular brain volumes. The vein fraction was calculated as the number of vein voxels in an ROI divided by the volume of the ROI. The vein counts were also calculated in various ROIs (WM, NAWM and WMHs) and were normalized to the periventricular volume. Limiting the analysis to the periventricular regions is due to two factors namely the high prevalence of WMHs in this area and lack of adequate image quality in the basal brain region on the SWI images.

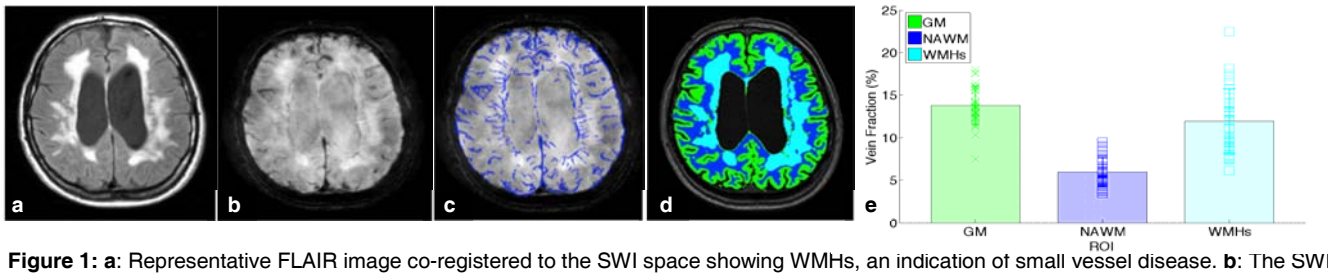

Figure 1: a: Representative FLAIR image co-registered to the SWI space showing WMHs, an indication of small vessel disease. **b**: The SWI image for the same participant showing the venous anatomy. **c**: Segmented venous structures overlaid on the SWI image. **d:** Tissue segmentation delineating GM (green), NAWM (blue) and WMHs (light blue). **e:** Vein fraction in different tissue ROIs.

Results: Lesion burden is reported as the percentage of the ROI that contains WMHs. An ROI analysis shows a higher vein fraction in the WMH lesion compared to NAWM as seen in Fig. 1.e (p<0.001). The vein fraction in the periventricular WM shows a positive correlation (p<0.05) (Fig. 2, top). We further consider the WMHs and NAWM and investigate the normalized vein count in each region. The vein count (#/volume) within the lesion was highly correlated with the SVD lesion burden (%) (p<0.001), but this was not the case for the vein count from voxels considered healthy deep white matter (p=0.328).

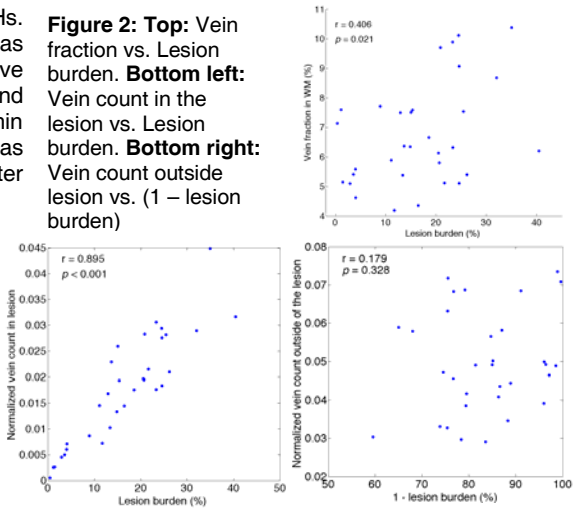

Figure 2: Top: Vein fraction vs. Lesion burden. **Bottom left:** Vein count in the lesion vs. Lesion burden. **Bottom right:** Vein count outside lesion vs. (1 – lesion burden)

Discussion and Conclusion: Our findings highlight the importance of investigating the venous vasculature in SVD. The higher vein fraction in WMHs compared to NAWM suggests the possible involvement of the venous vasculature in the etiology of the SVD. In fact, a limited number of pathological studies have identified the involvement of venous vasculature pathologies in WMHs [2, 9 & 10]. The positive correlation between the prominence of vein of the WM and the lesion load confirms our hypothesis and further supports the ischemic nature of SVD. On-going research involves integrating information available from SWI and arterial spin labeling perfusion imaging (data not shown).

References: [1] Thompson & Hakim, Stroke, 40(5):e322-30, 2009 [2] Brown & Thore, Neuropathol Appl Neurobiol, 37(1):56-74, 2011. [3] Haacke et al., AJNR, 30(2):232-52, 2009. [4] Ge et al., JMRI, 29(5):1190-4, 2009. [5] Arrigoni et al., AJNR, 32(11):2030-6, 2011. [6] Gibson et al., JMRI, 31(6):1311-22, 2010. [7] Frangi et al., MICCAI, 1496, 130-137, 1998. [8] Zhang et al., IEEE Trans Med Imag, 20(1):45-57, 2001. [9] Moody et al., Radiology, 194(2):469-76, 1995. [10] Black et al., Stroke, 40(3 Suppl):S48-52, 2009.